Efficient combinations of NOMA with distributed antenna systems based on channel measurements for mitigating jamming attacks

Joumana Farah, Eric Pierre Simon, Pierre Laly, Gauthier Delbarre

Efficient Combinations of NOMA with Distributed Antenna Systems based on Channel Measurements for Mitigating Jamming Attacks

Joumana Farah[1], Eric Pierre Simon[2], Pierre Laly[2], Gauthier Delbarre[2]

***Abstract*—This study aims at proposing new efficient combinations of distributed antenna systems (DAS) with non orthogonal multiple access (NOMA) for combating the influence of harmful jamming on a downlink transmission system. A large set of practical channel measurements was performed in an indoor work environment in order to encompass a wide panoply of user positions, antennas, and jammer configurations. Then, three strategies were studied for the selection of subbands, antennas and transmit powers so as to alleviate the influence of jamming. First, a configuration where the paired users are served by a unique antenna was considered. Then, two other configurations were studied, where paired users are served by two different antennas. It was shown that, in these two strategies, under specific channel and power conditions, it is possible to allow both paired users to perform successive interference cancellation (SIC) to remove inter-user interference. The dual-SIC strategy, when applied with joint antenna transmission, presents a good robustness to jamming and yields important throughput gains, compared to the classical single-SIC scenario and single-antenna dual-SIC transmission.**

***Index Terms*—NOMA, Distributed Antenna System, Antenna Selection, Subband Selection, Power Allocation, Channel Sounding.**

I. Introduction

Distributed antenna systems (DAS) have recently driven a large amount of research works [1]–[6], for leveraging the performance of wireless communication systems. DAS relies on the deployment of the base station antennas in a distributed manner in each cell, rather than on a single tower at the cell center. The remote antennas, or remote radio heads (RRH), are connected to a baseband unit (BBU) by fiber optics links. Compared to centralized antenna systems (CAS), DAS allows an important reduction of local electromagnetic radiations and CO2 emissions, enhanced antenna-users radio links, and a more uniform coverage throughout the area. The advantages of DAS can even be better reaped by its association with appropriate signal multiplexing, such as non orthogonal multiple access (NOMA) [7]–[11]. NOMA has shown to be a prominent key in the upcoming generations of communication systems, for its high potentials in boosting the spectral efficiency and user fairness, as well as in reducing latency [12], compared to orthogonal multiple access (OMA) used in the fourth generation of mobile systems. Power-domain NOMA consists on multiplexing two or more users on the same frequency subband by allocating different power levels to users, based on their channel gains. At the receivers side, user separation, when possible, is performed using successive interference cancellation (SIC). To perform SIC, a user extracts its own signal by successively demodulating, decoding then re-encoding and subtracting the successively detected interfering signals, before proceeding to the demodulation and decoding of its own intended signal. Users that are not able to perform SIC directly proceed to their signal decoding, while treating other interfering signals as noise. Therefore, two separate sets of conditions are to be studied for the feasibility of NOMA [13] [14]: first, the conditions on the achievable rates at the respective users levels, from the information theory perspective, leading to the so-called SIC constraints. Then, the constraints on the received signals powers that allow the SIC applicability from a practical implementation perspective, called power multiplexing constraints (PMC): the signal to be decoded at a certain level must have a received power greater than that of all other interfering signals on the same subband, in order to guaranty SIC stability [15].

A few previous works have tackled the combination of NOMA with DAS. In [16], the outage probability of a NOMA-based cloud radio access network (C-RAN) is studied for the case of two users, both served by all RRHs. The results show the superiority of NOMA when compared to time division multiple access (TDMA). The work in [17] investigates the application of distributed NOMA for the uplink of a partially centralized C-RANs. In [18] [19], resource allocation is studied in NOMA-DAS for the context of mixed-traffic users. In [14], subband and power allocation in NOMA-DAS was tackled for the minimization of the downlink cell power under fixed user rates, and the study was then adapted to incorporate hybrid RRH-specific power constraints in [20]. It was shown that, under specific SIC and PMC contraints, when the signals multiplexed on the same subband are sent from different RRHs, paired users can all cancel their respective interference, leading to the so-called "mutual SIC" (or "dual SIC" for the case of 2 users per subband). The latter was also applied for enhancing the spectral efficiency of Coordinated Multipoint (CoMP) systems [13]. However, none of these previous studies considered the impact of jamming on NOMA-DAS.

The jamming attacks consist in emitting a signal that covers the frequency bands employed by a wireless communication

J. Farah is with the Department of Electricity and Electronics, Faculty of Engineering, Lebanese University, Roumieh, Lebanon. e-mail: joumana-farah@ul.edu.lb. This work has been funded with support from the Lebanese University.

E.P. Simon, P. Laly and G. Delbarre are with the University of Lille and IEMN lab, Villeneuve d'Ascq, France. E.P. Simon is also a member of IRCICA. e-mail: eric.simon@univ-lille.fr; pierre.laly@univ-lille1.fr; gauthier.delbarre@univ-lille.fr

system in order to decrease the signal to noise ratio at the reception, leading to the degradation or disruption of the communication. This was shown in [21], where the impact of jamming on the performance of a IEEE 802.11n wireless network was analyzed. Different types of jammers exist, ranging from high-powered devices used by the army to low-powered devices which are portable and phone-sized. These low-powered devices are the most widespread due to their low price and the fact that they are easily accessible to everyone on the Internet. For these reasons, they constitute a real threat that has to be taken into account when deploying a wireless communication system [22]. One aspect of low-powered jammers that has to be taken into consideration is the fact that they are very easily transportable, so they can be deployed anywhere. To address this problem, various jamming deployments will be considered in this study, and proper resource allocation techniques will be proposed to combat its influence on the system performance.

The only previous work that considered jamming in the NOMA-DAS context is [23]. The authors considered the energy-efficiency of DAS using classical single-SIC NOMA (where only one paired user can perform SIC), to alleviate the influence of a reactive jammer, by using statistical observations of the jammer behaviour.

Moreover, the incorporation of realistic channel measurements in the resource allocation, as was done in [24] for multi-antenna beamforming, provides a better insight into the strategies that should be adopted for optimizing system performance.

To the best of our knowledge, this is the first work that proposes the optimization of several pairing scenarios in the NOMA-DAS context, in the presence of jamming, and by incorporating channel measurements. The main contributions of this work can be summarized as follows:

- We introduce three different user-pairing strategies combined with RRH and subband selection for counteracting the influence of jamming in a NOMA-DAS system.
- We determine the necessary conditions for allowing inter-user interference cancellation in downlink NOMA in the presence of jamming, for each of the three scenarios.
- We show that, under specific conditions, it is possible to allow both paired users on a subband to perform SIC in order to remove their mutual interference.
- We base our performance analysis on practical channel measurements that allow us to draw interesting conclusions concerning the best transmission strategies to adopt depending on the users and jammer positions in the cell. We also show how the best user-antenna association and subband selection that optimize the system capacity can be adapted to the users and jammer positions.

The paper is organized as follows: In Section II, the NOMA-DAS system model is given with the proposed user-pairing scenarios. In Section III, we describe the measurement setup and environment. Then, in Section IV, we develop the SIC and PMC conditions for each user-pairing scenario. The proposed antenna and frequency selection technique is described in Section V. Performance evaluation of the resource allocation techniques is provided in Section VI, while Section VII concludes the paper.

II. System Model

The system is modeled by a downlink transmission system where R single-antenna RRHs, linked to a BBU, are deployed over the geographical area, as shown in Fig. 1. Two users k_1 and k_2 are randomly positioned in the considered area. These users can be mobile cellular transceivers or IoT devices. The overall system bandwidth B is divided into S equal subbands, where each subband is an integer number of OFDM (Orthogonal Frequency Division Multiplexing) subcarriers. A jammer J, positioned at a random unknown location, jams all transmitted signals with equal power. The RRHs constitue a set $\mathcal{R} = \{1, ..., R\}$. In what follows, since a single subband is considered at a time, for the sake of simplicity, we do not include a subband index in the channel gains and power variables. Let:

- $h_{k,r}$ the channel gain between RRH r and user k,
- $h_{k,J}$ the channel gain between the jammer and user k,
- $P_{k,r}$ the power allocated by the BBU for the transmission of the signal from RRH r to user k,
- P_J the transmit power of the jammer.

The channel gains between the users and the RRHs need to be known at the level of the network entity that is responsible for performing RRH, subband and power allocation to serve users. In the DAS context, the BBU constitutes this entity. In the case of Frequency Division Duplex (FDD), where uplink and downlink transmissions occur on different frequencies, each user is assumed to periodically perform channel estimation using pilot signals received from the RRHs. Channel state information (CSI) on the RRH-user channel responses is then transmitted back from the users to the BBU via the RRHs. By collecting this information, the BBU can then perform proper resource allocation. In a Time Division Duplex (TDD) context, where uplink and downlink transmissions are time-multiplexed on the same frequencies, channel reciprocity can be exploited so that the estimation of the user-RRH channel responses can be directly conducted at the RRH level, thereby avoiding the need for signaling CSI information from the users to the BBU. In this work, perfect knowledge of the RRH-user channel gains by the BBU is assumed.

As for the jamming power P_J and the channel gains $h_{k,J}$, they are unknown to the BBU. However, each user regularly measures its received signal levels on the different frequencies and signals them to the RRHs. The BBU can therefore compare these signal levels with the ones expected to be experienced at each user in the absence of jamming. Based on this comparison, the BBU can estimate $P_J h_{k,J}$, the received jamming power at each user level.

Two transmission scenarios were studied in DAS [25], [26]: selection diversity and blanket transmission. In the first, only one of the RRHs is selected for the transmission of a signal, whereas in the second, all RRHs participate in each transmission, thus creating a macroscopic multi-antenna system. It was found that selection diversity achieves a better system capacity than blanket transmission. Therefore, in this

study, a maximum of 2 RRHs are adaptively chosen to serve the paired users k_1 and k_2 on a subband. k_1 and k_2 are either served by the same RRH, as in Fig. 1a, or by two different RRHs, as in Fig. 1b. The first case will be referred to as single-SIC NOMA, since, as will be shown mathematically, when a unique RRH serves both paired users, only one of the latter can perform SIC. In the second case, two RRHs are used to transmit the two signals, leading to the possibility of both users performing SIC.

The conditions to allow dual-SIC NOMA were developed in [13] and [14] for the case of a jamming-free system. In this study, we develop these conditions for the jammed system, and show that even in the presence of jamming, dual-SIC is still possible, even though with harsher conditions. The dual-SIC case actually encloses two different possible scenarios: in the first one, referred to as dual-SIC NOMA with single-antenna transmission, each user receives its signal via one of the two involved RRHs only. In the second, referred to as dual-SIC NOMA with joint-antenna transmission, the signal of each user is jointly transmitted by both involved RRHs.

Let $s_{k,r}$ be the signal transmitted from RRH r to user k with power $P_{k,r}$. Note that, since only two users are considered for pairing on a subband, in the sequel, the indices k_1 and k_2 are respectively replaced by 1 and 2 in the power and channel variables. In the Single-SIC scenario, since the same RRH r transmits the signals of both paired users k_1 and k_2, the transmitted power-multiplexed signal is expressed by:

$$x = \sum_{i=1}^{2} \sqrt{P_{i,r}} s_{i,r}, \tag{1}$$

where $E[|s_{i,r}|^2] = 1$, $i = 1, 2$. The signal received at the level of each user can be written as:

$$y_i = h_{i,r} x + h_{i,J} \sqrt{P_J} s_J + n_i, i = 1, 2, \tag{2}$$

where s_J is the signal transmitted by the jammer ($E[|s_J|^2] = 1$) and n_i is an i.i.d. additive white Gaussian noise (AWGN) with zero mean and variance $\sigma^2 = N_0 B/S$, where N_0 is the noise power spectral density.

When dual-SIC NOMA with single-antenna transmission is used, the signal transmitted by RRH r_i (the RRH powering the signal of user i) is written as:

$$x_i = \sqrt{P_{i,r_i}} s_{i,r_i}, \tag{3}$$

and the signal received by user i is now:

$$y_i = \sum_{j=1}^{2} h_{i,r_j} x_j + h_{i,J} \sqrt{P_J} s_J + n_i, i = 1, 2. \tag{4}$$

When the third transmission scenario is considered, i.e., dual-SIC NOMA with joint-antenna transmission, (3) and (4) are replaced by:

$$x_i = \sum_{j=1}^{2} \sqrt{P_{j,r_i}} s_{j,r_i}, \tag{5}$$

and

$$y_i = \sum_{j=1}^{2} h_{i,r_j} x_j + h_{i,J} \sqrt{P_J} s_J + n_i, i = 1, 2, \tag{6}$$

The aim of this study is to dynamically select the best RRH (or couple of RRHs, depending on the pairing scenario) and subband, on which the two users k_1 and k_2 are paired, in such a way to maximize their sum-throughput, while taking into account the jammer presence. To this aim, after a detailed description of the channel measurements and a thorough study of the conditions inherent to the different user pairing scenarios, a novel RRH and subband selection technique is proposed in Section V. Also, the extension of the study to the multi-user pairing case is discussed therein.

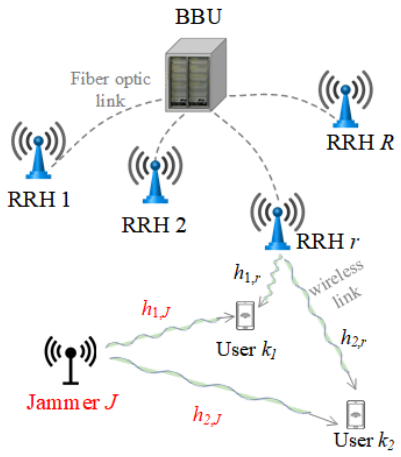

(a) Single-SIC NOMA

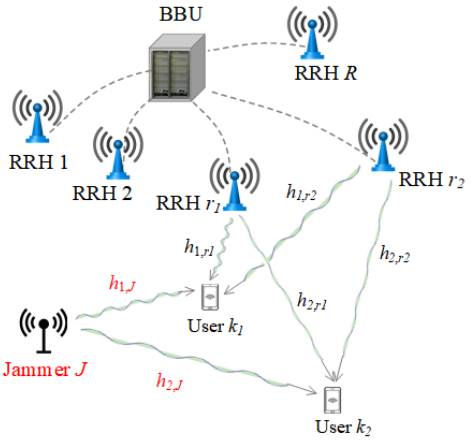

(b) Dual-SIC NOMA

Fig. 1: System model of DAS under jamming attack.

III. Description of the Measurements

In this section, we present the measurement campaign performed in the DAS context, on which we base our study to assess the different NOMA pairing combinations. We start by introducing the measurement equipment. Then, we describe the environment where measurements are carried out.

A. Measurement setup

Frequency-domain channel sounding measurements are performed in an indoor environment. A vector network analyzer (VNA) of type Agilent Technologies E5071C is used to sound the radio channel in an 18 MHz bandwidth centered at 3.5 GHz. In this frequency band, 1200 uniformly spaced frequency points, i.e., OFDM subcarriers, are sampled with a frequency spacing of 15 KHz, corresponding to the LTE/LTE Advanced mobile system parameters [27]. Each group of contiguous subcarriers constitutes one subband, which will be the basis of resource allocation in the following sections. The feeder cables used for the transmit and receive antennas are MegaPhase high performance RF coaxial cables. They are included in the VNA calibration to cancel their effect in the channel sounder. For each measurement, the VNA acquires 10 successive realizations of the whole frequency range, which are then averaged for the reduction of measurement noise. The transmitter is equipped with a patch antenna positioned at a height of 2m above ground level. The receiver is equipped with a EM-6116 omnidirectional antenna at 1.50m. Fig. 2 shows the transmitter and receiver in the considered environment.

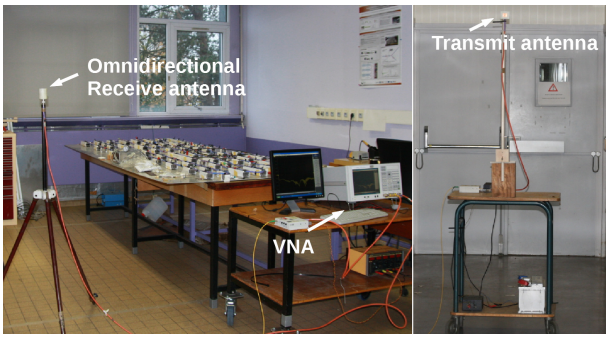

Fig. 2: Practical setup for channel measurements

B. Measurement Environment

The measurements were conducted in the first floor of a typical indoor building, consisting of two rows of offices and laboratories, situated on both sides of a 35m long corridor. A map of the environment is shown in Fig. 3. All offices and lab rooms are separated by plaster walls, except for two concrete walls shown in the figure. The channels were sounded in the corridor (numbered #1) and 11 different selected rooms, numbered from #2 to #12. The set of measurements is obtained by moving the transmitter and receiver at different positions to constitute a DAS. Each position of the transmitter corresponds to an RRH, and each position of the receiver corresponds to a given user (U). The positions of the RRHs and users are specified as follows: a first index i identifies the room, and a second index j indicates the position within this room, yielding RRHij and Uij. The orientation of the RRH patch antenna is shown by arrows. In order to investigate several scenarios with different jammer positions, five of the transmitter positions are dedicated to the jammer (J) and spotted in red in Fig. 3.

IV. Analysis of the User-Pairing Scenarios

In this section, we derive the SIC conditions and power multiplexing constraints for the three user pairing scenarios: Single-SIC, dual-SIC with single antenna transmission, and dual-SIC with joint antenna transmission.

A. Single-SIC NOMA

In this first scenario, the signals of the two paired users k_1 and k_2, denoted respectively by s_1 and s_2 for simplicity, are transmitted by the same RRH $r \in \mathcal{R}$.
Let $SINR_{s_2}^{(k_1)}$ the necessary Signal to Interference and Noise Ratio (SINR) at the level of user k_1 for decoding the signal s_2 of k_2. It is expressed as:

$$SINR_{s_2}^{(k_1)} = \frac{P_{2,r}h_{1,r}}{P_{1,r}h_{1,r} + P_J h_{1,J} + \sigma^2}. \quad (7)$$

Similarly, let $SINR_{s_2}^{(k_2)}$ the necessary SINR at the level of user k_2 for decoding s_2. It is given by:

$$SINR_{s_2}^{(k_2)} = \frac{P_{2,r}h_{2,r}}{P_{1,r}h_{2,r} + P_J h_{2,J} + \sigma^2}. \quad (8)$$

It is known, from the theory behind NOMA [8] [13] [14], that k_1 can successfully decode and cancel the interfering signal s_2 if:

$$SINR_{s_2}^{(k_1)} \geq SINR_{s_2}^{(k_2)}. \quad (9)$$

By developing and arranging $SINR_{s_2}^{(k_1)} - SINR_{s_2}^{(k_2)}$, it can be verified that (9) leads to the following condition:

$$P_J P_{2,r}(h_{1,r}h_{2,J} - h_{2,r}h_{1,J}) + \sigma^2 P_{2,r}(h_{1,r} - h_{2,r}) \geq 0. \quad (10)$$

Since, in practical interference-limited systems, additive noise is generally negligible with respect to interfering signals, the second term in (10) is negligible towards the first; therefore, (10) reduces to:

$$h_{1,r}h_{2,J} \geq h_{2,r}h_{1,J}. \quad (11)$$

From the practical perspective, in order to ensure SIC stability, i.e. minimize the chances of error propagation in SIC, since signal s_2 is to be decoded first, it must be the dominant one so that the receiver of k_1 can distinguish it from interference and background noise. In the presence of jamming, if the received power of s_1 and that of the jammer's signal s_J add up to a more powerful combined signal at k_1, their resulting interference will become dominant with respect to the signal s_2 received by k_1, therefore threatening its successful decoding. For this reason, the PMC for the decoding of s_2 at the level of k_1 is:

$$P_{2,r}h_{1,r} \geq P_{1,r}h_{1,r} + P_J h_{1,J}. \quad (12)$$

Using the same reasoning, by interchanging k_1, k_2 and s_1, s_2 in (7), (8), (9), and (10), it can be verified that k_2 can successfully decode and cancel the signal s_1 if:

$$h_{2,r}h_{1,J} \geq h_{1,r}h_{2,J}. \quad (13)$$

Consequently, it is clear that when conditions (11) and (12) are verified, only user k_1 can perform SIC, i.e., k_2 cannot. In

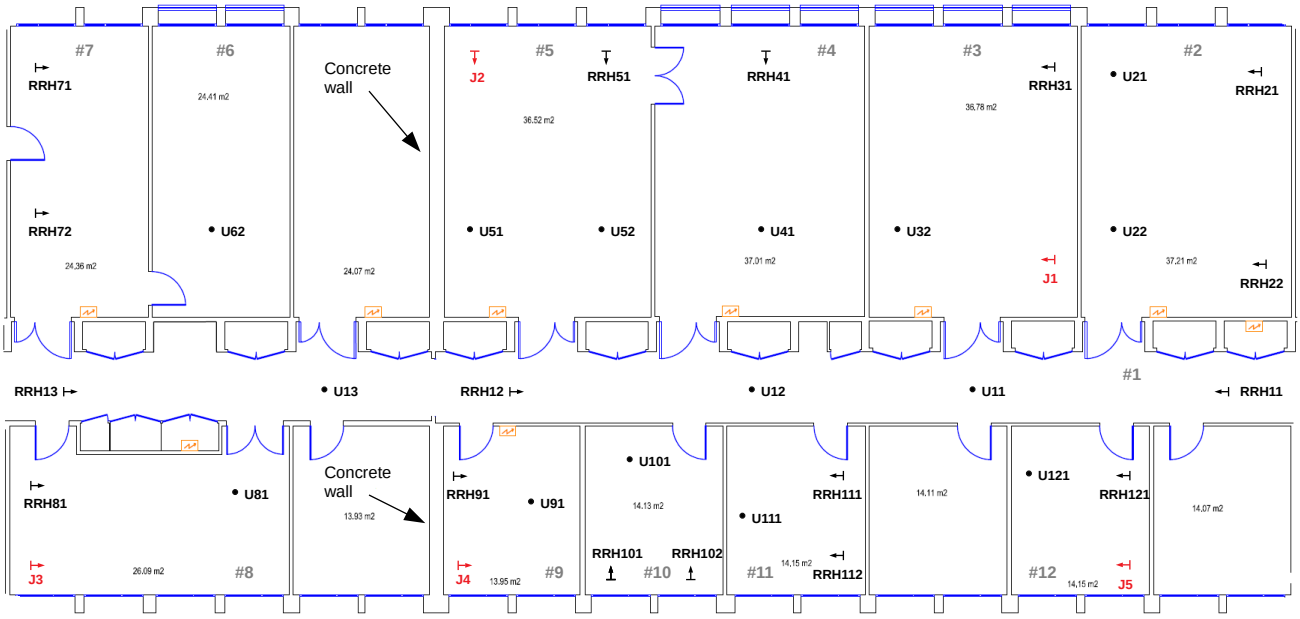

Fig. 3: Measurement Environment

this case, the normalized rates (spectral efficiencies) achieved by the two users are respectively:

$$R_{k_1} = \log_2(1 + \frac{P_{1,r}h_{1,r}}{P_J h_{1,J} + \sigma^2}), \tag{14}$$

$$R_{k_2} = \log_2(1 + \frac{P_{2,r}h_{2,r}}{P_{1,r}h_{2,r} + P_J h_{2,J} + \sigma^2}). \tag{15}$$

When (13) is verified, k_2 performs SIC, while k_1 does not. The corresponding PMC becomes:

$$P_{1,r}h_{2,r} \geq P_{2,r}h_{2,r} + P_J h_{2,J}. \tag{16}$$

The achieved rates are in this case:

$$R_{k_1} = \log_2(1 + \frac{P_{1,r}h_{1,r}}{P_{2,r}h_{1,r} + P_J h_{1,J} + \sigma^2}), \tag{17}$$

$$R_{k_2} = \log_2(1 + \frac{P_{2,r}h_{2,r}}{P_J h_{2,J} + \sigma^2}). \tag{18}$$

Note that when $P_J = 0$, conditions (10) and (12) reduce respectively to $h_{1,r} \geq h_{2,r}$ and $P_{2,r} \geq P_{1,r}$, which correspond to the SIC and PMC conditions in the classical jamming-free NOMA transmission [7] [8]. Also, the rates in equations (14), (15), (17), (18) become devoid of the jamming power terms. In practice, based on the received measurements of $P_J h_{1,J}$ and $P_J h_{2,J}$ (as explained in Section II), the BBU calculates the ratio: $h_{2,J}/h_{1,J} = P_J h_{2,J}/P_J h_{2,J}$. If $h_{2,J}/h_{1,J} \geq h_{2,r}/h_{1,r}$, the BBU performs power allocation while considering k_1 as the strong user on the considered subband, i.e., the user performing SIC, and k_2 as the weak user. Otherwise, k_2 is considered as the strong user.

B. Dual-SIC NOMA with Single Antenna Transmission (Dual-SIC-SAT)

In this pairing scenario, the two users k_1 and k_2 receive their signals s_1 and s_2 from two different RRHs $r_1 \in \mathcal{R}$ and $r_2 \in \mathcal{R}$, respectively, as shown in Fig. 1b. Only one selected RRH participates to transmit a user's signal. In [14], where such a transmission scenario was studied in the absence of jamming, it was shown that, under specific channel and transmit power conditions, both users k_1 and k_2 are able to perform SIC to cancel their respective signals. The question that arises now is whether this mutual SIC can still take place in spite of the jamming, and if yes, under which conditions. In this scenario, the SINR expressions in (7) and (8) become respectively:

$$SINR_{s_2}^{(k_1)} = \frac{P_{2,r_2}h_{1,r_2}}{P_{1,r_1}h_{1,r_1} + P_J h_{1,J} + \sigma^2}, \tag{19}$$

$$SINR_{s_2}^{(k_2)} = \frac{P_{2,r_2}h_{2,r_2}}{P_{1,r_1}h_{2,r_1} + P_J h_{2,J} + \sigma^2}. \tag{20}$$

k_1 can perform SIC if the inequality $SINR_{s_2}^{(k_1)} - SINR_{s_2}^{(k_2)} \geq 0$ holds. After rearranging its terms and neglecting the additive noise, this inequality is shown to be equivalent to:

$$\begin{aligned} &P_{1,r_1}P_{2,r_2}\underbrace{(h_{1,r_2}h_{2,r_1} - h_{1,r_1}h_{2,r_2})}_{E} + \\ &P_{2,r_2}P_J\underbrace{(h_{1,r_2}h_{2,J} - h_{2,r_2}h_{1,J})}_{F} \geq 0. \end{aligned} \tag{21}$$

The condition for k_2 to perform SIC is $SINR_{s_1}^{(k_2)} - SINR_{s_1}^{(k_1)} \geq 0$, which leads to:

$$\begin{aligned} &P_{1,r_1}P_{2,r_2}\underbrace{(h_{1,r_2}h_{2,r_1} - h_{1,r_1}h_{2,r_2})}_{E} + \\ &P_{1,r_1}P_J\underbrace{(h_{2,r_1}h_{1,J} - h_{1,r_1}h_{2,J})}_{G} \geq 0. \end{aligned} \tag{22}$$

Note that, if the common factor E in (21) and (22) is negative, i.e.,

$$\frac{h_{2,r_1}}{h_{1,r_1}} \leq \frac{h_{2,r_2}}{h_{1,r_2}},$$

F and G cannot be simultaneously positive, since:

$$(F \geq 0)\&(G \geq 0) \iff \left(\frac{h_{2,J}}{h_{1,J}} \geq \frac{h_{2,r_2}}{h_{1,r_2}}\right)\&\left(\frac{h_{2,J}}{h_{1,J}} \leq \frac{h_{2,r_1}}{h_{1,r_1}}\right) \iff \frac{h_{2,r_2}}{h_{1,r_2}} \leq \frac{h_{2,J}}{h_{1,J}} \leq \frac{h_{2,r_1}}{h_{1,r_1}}. \quad (23)$$

In other words, if $E \leq 0$, dual SIC between k_1 and k_2 is not possible. Conversely, if

$$\frac{h_{2,r_2}}{h_{1,r_2}} \leq \frac{h_{2,r_1}}{h_{1,r_1}}, \quad (24)$$

then (23) can be true, under specific jamming conditions.
Also, when $P_J = 0$, by inspecting (21) and (22), one can see that the dual SIC condition between k_1 and k_2 simply reduces to condition (24), as was the case in [14].

The PMCs at the levels of users k_1 and k_2 are respectively:

$$P_{2,r_2}h_{1,r_2} \geq P_{1,r_1}h_{1,r_1} + P_J h_{1,J},$$
$$P_{1,r_1}h_{2,r_1} \geq P_{2,r_2}h_{2,r_2} + P_J h_{2,J}.$$

The two above PMCs can be combined into the following one:

$$\frac{h_{1,r_1}}{h_{1,r_2}} + \frac{P_J h_{1,J}}{P_{1,r_1}h_{1,r_2}} \leq \frac{P_{2,r_2}}{P_{1,r_1}} \leq \frac{h_{2,r_1}}{h_{2,r_2}} - \frac{P_J h_{2,J}}{P_{1,r_1}h_{2,r_2}}. \quad (25)$$

When $P_J = 0$, (25) becomes simply:

$$\frac{h_{1,r_1}}{h_{1,r_2}} \leq \frac{P_{2,r_2}}{P_{1,r_1}} \leq \frac{h_{2,r_1}}{h_{2,r_2}}, \quad (26)$$

which corresponds to the jamming-free context [14]. More importantly, when inspecting (24) and (26), it can be clearly seen that, in the jamming-free case, when (24) is not verified, i.e. dual SIC is not possible between k_1 and k_2 with the current antenna selection (resp. r_1 and r_2), a simple RRH inversion is sufficient to enable dual SIC, i.e. k_1 is served by r_2 and k_2 by r_1. Unfortunately, this is no longer true in the presence of jamming, as shown by (23) and (25). In other words, when (24) is not verified, while $P_J \neq 0$, one can still consider inverting the RRHs to enlarge the ensemble of tested RRH pairs. However, there is no guarantee that this inversion will lead to a valid RRH pair. Finally, when (23) and (25) are both respected, the achieved user rates are:

$$R_{k_1} = \log_2(1 + \frac{P_{1,r_1}h_{1,r_1}}{P_J h_{1,J} + \sigma^2}), \quad (27)$$

$$R_{k_2} = \log_2(1 + \frac{P_{2,r_2}h_{2,r_2}}{P_J h_{2,J} + \sigma^2}). \quad (28)$$

C. Dual-SIC NOMA with Joint Antenna Transmission (Dual-SIC-JAT)

When joint transmission is considered on top of Dual-SIC NOMA, the two selected RRHs r_1 and r_2 participate in the transmission of each of the two signals addressed to k_1 and k_2. In this case, the SINR expressions become:

$$SINR_{s_2}^{(k_1)} = \frac{P_{2,r_1}h_{1,r_1} + P_{2,r_2}h_{1,r_2}}{P_{1,r_1}h_{1,r_1} + P_{1,r_2}h_{1,r_2} + P_J h_{1,J} + \sigma^2}, \quad (29)$$

$$SINR_{s_2}^{(k_2)} = \frac{P_{2,r_1}h_{2,r_1} + P_{2,r_2}h_{2,r_2}}{P_{1,r_1}h_{2,r_1} + P_{1,r_2}h_{2,r_2} + P_J h_{2,J} + \sigma^2}. \quad (30)$$

The condition $SINR_{s_2}^{(k_1)} - SINR_{s_2}^{(k_2)} \geq 0$, necessary for k_1 to perform SIC, amounts to:

$$\begin{aligned}(h_{1,r_1}h_{2,r_2} - h_{1,r_2}h_{2,r_1})(P_{2,r_1}P_{1,r_2} - P_{2,r_2}P_{1,r_1}) \\ +P_J \underbrace{(P_{2,r_1}h_{1,r_1} + P_{2,r_2}h_{1,r_2})}_{A(P)} h_{2,J} \\ -P_J \underbrace{(P_{2,r_1}h_{2,r_1} + P_{2,r_2}h_{2,r_2})}_{B(P)} h_{1,J} \geq 0.\end{aligned} \quad (31)$$

Also, the necessary condition for k_2 to perform SIC is:

$$\begin{aligned}(h_{2,r_1}h_{1,r_2} - h_{2,r_2}h_{1,r_1})(P_{1,r_1}P_{2,r_2} - P_{1,r_2}P_{2,r_1}) \\ +P_J \underbrace{(P_{1,r_1}h_{2,r_1} + P_{1,r_2}h_{2,r_2})}_{C(P)} h_{1,J} \\ -P_J \underbrace{(P_{1,r_1}h_{1,r_1} + P_{1,r_2}h_{1,r_2})}_{D(P)} h_{2,J} \geq 0.\end{aligned} \quad (32)$$

The PMCs at the level of users k_1 and k_2 are respectively:

$$P_{2,r_1}h_{1,r_1} + P_{2,r_2}h_{1,r_2} \geq P_{1,r_1}h_{1,r_1} + P_{1,r_2}h_{1,r_2} + P_J h_{1,J}, \quad (33)$$

$$P_{1,r_1}h_{2,r_1} + P_{1,r_2}h_{2,r_2} \geq P_{2,r_1}h_{2,r_1} + P_{2,r_2}h_{2,r_2} + P_J h_{2,J}. \quad (34)$$

It is therefore clear that any power allocation scheme must abide by the four constraints (31), (32), (33) and (34), since they all include power variables. However, the SIC constraints (31) and (32) are non linear in $P_{k,r}$, which may hinder the problem feasibility. For this sake, in the sequel, we propose a simplification of the constraints.

The PMCs (33) and (34) can be rewritten as:

$$(P_{2,r_2} - P_{1,r_2})h_{1,r_2} \geq (P_{1,r_1} - P_{2,r_1})h_{1,r_1} + P_J h_{1,J}, \quad (35)$$

$$(P_{1,r_1} - P_{2,r_1})h_{2,r_1} \geq (P_{2,r_2} - P_{1,r_2})h_{2,r_2} + P_J h_{2,J}. \quad (36)$$

By inspecting (35) and (36), it can be deduced that the factors $P_{1,r_1} - P_{2,r_1}$ and $P_{2,r_2} - P_{1,r_2}$ always have the same sign. When $P_{1,r_1} - P_{2,r_1} \geq 0$ and $P_{2,r_2} - P_{1,r_2} \geq 0$, $P_{1,r_1}P_{2,r_2} \geq P_{2,r_1}P_{1,r_2}$. Also, (35) and (36) combine to:

$$\frac{h_{2,r_2}}{h_{2,r_1}} + \frac{P_J h_{2,J}}{h_{2,r_1}(P_{2,r_2} - P_{1,r_2})} \leq \frac{P_{1,r_1} - P_{2,r_1}}{P_{2,r_2} - P_{1,r_2}} \leq \frac{h_{1,r_2}}{h_{1,r_1}} - \frac{P_J h_{1,J}}{h_{1,r_1}(P_{2,r_2} - P_{1,r_2})}.$$

Consequently, when the PMCs (33) and (34) are verified, $h_{2,r_2}/h_{2,r_1} \leq h_{1,r_2}/h_{1,r_1}$, and since $P_{2,r_1}P_{1,r_2} - P_{1,r_1}P_{2,r_2} \leq 0$, the common term $(h_{1,r_1}h_{2,r_2} - h_{1,r_2}h_{2,r_1})(P_{2,r_1}P_{1,r_2} - P_{2,r_2}P_{1,r_1})$ in (31) and (32) is positive.
Similarly, when $P_{1,r_1} - P_{2,r_1} \leq 0$ and $P_{2,r_2} - P_{1,r_2} \leq 0$, $P_{1,r_1}P_{2,r_2} \leq P_{2,r_1}P_{1,r_2}$, (35) and (36) combine to:

$$\frac{h_{1,r_2}}{h_{1,r_1}} - \frac{P_J h_{1,J}}{h_{1,r_1}(P_{2,r_2} - P_{1,r_2})} \leq \frac{P_{1,r_1} - P_{2,r_1}}{P_{2,r_2} - P_{1,r_2}} \leq \frac{h_{2,r_2}}{h_{2,r_1}} + \frac{P_J h_{2,J}}{h_{2,r_1}(P_{2,r_2} - P_{1,r_2})}.$$

This leads to $h_{1,r_2}/h_{1,r_1} \leq h_{2,r_2}/h_{2,r_1}$, and since $P_{2,r_1}P_{1,r_2} - P_{1,r_1}P_{2,r_2} \geq 0$, the common term in (31) and (32) is also positive. Therefore, based on the positivity of this common

term, it is removed from the PMC constraints, and the four constraints (31), (32), (33) and (34) are finally re-written as:

$$\begin{cases} A(P)h_{2,J} - B(P)h_{1,J} \geq 0, \\ C(P)h_{1,J} - D(P)h_{2,J} \geq 0, \\ A(P) - D(P) - P_J h_{1,J} \geq 0, \\ C(P) - B(P) - P_J h_{2,J} \geq 0. \end{cases} \tag{37}$$

$A(P)$, $B(P)$, $C(P)$ and $D(P)$ are linear functions of the power variables. Note that this simplification may reduce the search space of the power variables; however, the linearity of the constraints greatly counteracts this effect from the feasibility perspective.

When the constraints in (37) are verified, the achieved user rates are:

$$R_{k_1} = \log_2(1 + \frac{P_{1,r_1}h_{1,r_1} + P_{1,r_2}h_{1,r_2}}{P_J h_{1,J} + \sigma^2}), \tag{38}$$

$$R_{k_2} = \log_2(1 + \frac{P_{2,r_1}h_{2,r_1} + P_{2,r_2}h_{2,r_2}}{P_J h_{2,J} + \sigma^2}). \tag{39}$$

V. Antenna and Frequency Selection

The selection of the optimum transmitting RRH (or RRH couple) and subband, for a particular user couple, is highly dependent on the transmit powers. Therefore, we start by describing the power allocation (PA) strategy for each user pairing scenario. In the single-SIC NOMA scenario, the PA problem on a particular subband is expressed as:

$$\max_{\{P_{1,r}, P_{2,r}\}} R_{k_1} + R_{k_2}, \tag{40}$$

such that:

$$\begin{cases} \text{(12) verified (if (11) is true)} & \text{(40a)} \\ \text{or (16) verified (if (13) is true),} & \text{(40b)} \\ P_{1,r} + P_{2,r} \leq P_L. & \text{(40c)} \end{cases}$$

P_L is the maximum power budget of an RRH.

R_{k_1} and R_{k_2} are expressed by (14) and (15) respectively, if (11) is true, or by (17) and (18), respectively, if (13) is true.
In the dual-SIC NOMA with single antenna transmission scenario, when (23) is verified, the PA problem is formulated as:

$$\max_{\{P_{1,r_1}, P_{2,r_2}\}} R_{k_1} + R_{k_2}, \tag{41}$$

such that:

$$\begin{cases} \text{(25) verified,} & \text{(41a)} \\ P_{1,r_1} \leq P_L/2, & \text{(41b)} \\ P_{2,r_2} \leq P_L/2. & \text{(41c)} \end{cases}$$

R_{k_1} and R_{k_2} are now expressed by (27) and (28) respectively. As shown in constraints (41b) and (41c), the power budget of each involved RRH is set to $P_L/2$, so that the total power budget of the RRHs powering the subband is kept equal to that of the single RRH involved in the single-SIC scenario. This allows a fair comparison between the different pairing schemes.

When dual-SIC NOMA is applied with joint antenna transmission, the PA problem becomes:

$$\max_{\{P_{1,r_1}, P_{1,r_2}, P_{2,r_1}, P_{2,r_2}\}} R_{k_1} + R_{k_2}, \tag{42}$$

such that:

$$\begin{cases} \text{(37) verified,} & \text{(42a)} \\ P_{1,r_1} + P_{2,r_1} \leq P_L/2, & \text{(42b)} \\ P_{2,r_2} + P_{2,r_2} \leq P_L/2. & \text{(42c)} \end{cases}$$

R_{k_1} and R_{k_2} are given by (38) and (39) respectively.

We now move to the description of the general strategy for subband and RRH selection, for a couple of users k_1 and k_2. In the case of single-SIC NOMA, any couple (r,s) of RRH r and subband s either verifies (11) or (13), and thus constitutes a possible candidate. Therefore, problem (40) is resolved for each couple (r,s). The couple that yields the highest throughput is then used to serve k_1 and k_2.
In Dual-SIC NOMA with single antenna transmission, only the triplets (r_1,r_2,s), with $r_1 \neq r_2$, and verifying (23), are tested by resolving problem (41). k_1 and k_2 are then assigned the triplet (r_1,r_2,s) that yield the maximum throughput.
When joint antenna transmission is considered with Dual-SIC NOMA, problem (42) is resolved for all triplets (r_1,r_2,s) such that $r_1 \neq r_2$. Note that, in the three user pairing strategies, some of the candidates (r,s) or (r_1,r_2,s) do not yield valid solutions (i.e. the PA constraints cannot be met with positive power variables) and are eliminated. Also, the PA in Dual-SIC-JAT generally necessitates a higher complexity than that of Dual-SIC-SAT and Single-SIC, since four power variables are to be determined instead of two.

To determine the solution of each one of the problems (40), (41) and (42), one could use Lagrangian optimization. However, since multi-constraint problems with non-linear objective functions are at stake, we directly resort to the use of the Optimization Toolbox in Matlab to find the power allocation solutions.
Note that, while we focused our study on a particular user pair, in a practical system a large number of active users are generally present. Therefore, different user pairs are assigned separate subbands powered by one or two RRHs. Moreover, each user position considered in the channel measurements conducted in our study can be considered as a different user in a multi-user system. Such setup would be a generalization of the current study, where an assignment algorithm needs to be implemented to jointly perform user pairing, RRH and subband selection, and power allocation to all active users. Such a complete solution can be implemented by incorporating, within the current study, either a greedy algorithm [14] or a matching technique [19], in the DAS context. However, this is out of the scope of the current study, where the main focus is on the best RRH-subband selection to counteract the jamming effect.
The study, conducted in this work for the case of two-user clusters, can be extended to larger cluster sizes. For instance, if one considers clusters of three users per subband, mutual SIC between all cluster members would require two SIC processes at each user level (to cancel the interference of each of the two respective users), with two corresponding PMCs. This would amount to a total of 12 constraints instead of 4 in (37). Also, for each possible RRH and subband candidate, 8 decoding

orders need to be tested at the BBU (2 at the level of each user). The one that yields the best sum-throughput is then signaled by the BBU to the users through the RRHs. As was shown in [13], by the complete mutual SIC, and in contrast with traditional SIC procedures (where clustered users' signals are powered by a unique RRH), successfully adding a user to a NOMA cluster is virtually equivalent to enlarging the system bandwidth. Therefore, a greater number of accommodated users per subband will translate into a higher performance in mutual SIC systems. However, this enlargement incurs a significant increase in complexity at the BBU level as well as at the user equipment levels, with a higher risk of error propagation at the SIC receivers. For all these reasons, we chose to limit the cluster size to two in this study. However, its extension to larger clusters could constitute an interesting perspective to be investigated in a future work.

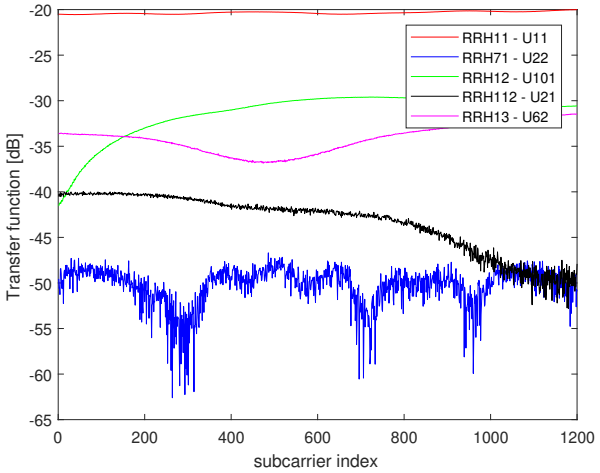

Fig. 4: Examples of measured transfer functions

VI. Performance Evaluation

The different resource allocation methods presented in this study are evaluated for the case of S = 12 subbands, where each subband is equivalent to 100 OFDM subcarriers. The noise power spectral density is $N_0 = 4 \times 10^{-18}$ mW/Hz. For each possible user couple (k_1, k_2), the antenna and frequency selection technique is applied separately for each of the three DAS-NOMA pairing scenarios.

Fig. 4 shows examples of the measured transfer functions for five different combinations of users and RRHs. As expected, when the transmitter and receiver are in the same room (red curve), the line of sight dominates in the signal transmission which yields an almost flat transfer function with a high amplitude. The blue curve corresponds to the case where the transmitter and receiver are at the opposite ends of a row of rooms. In this case, besides suffering the large distance, the signal has to cross the concrete walls, yielding low amplitudes and highly frequency-selective fading. The black curve also corresponds to a scenario giving low channel amplitudes, where the transmitter antenna points towards the opposite direction of the receiver (see Fig. 3). The green and magenta curves correspond to a more moderate fading in comparison to the blue and black curves, since the user and transmitter are taken in separate but close rooms.

In Fig. 5, we represent the sum-throughput $(R_{k_1} + R_{k_2})$ averaged over all possible user couples considered in the study, while variating the jamming power P_J, for the case of a total transmit power P_L = 1W. The results show that, for a low jamming power (smaller than 1mW), both dual SIC strategies outperform Single-SIC. This observation is in line with the results obtained in [13] [14] in the jamming-free context. However, when P_J increases, Single-SIC outperforms Dual-SIC-SAT with a throughput gain that can reach 7.7 bps/Hz at P_J = 10W. The quick performance degradation of Dual-SIC-SAT can be mainly explained by the subtractive term in the right-hand part of inequation (25): When P_J increases, this constraint becomes very hard to respect, which hinders the feasibility of problem (41). Therefore, the number of valid candidate antennas and subbands decreases quickly with P_J. At the same time, constraints (12) and (16) are easier to respect, leading to a higher number of possible candidates in Single-SIC. As for Dual-SIC-JAT, it constitutes the best user pairing strategy, with a good immunity to jamming power. Indeed, it outperforms both Single-SIC and Dual-SIC-SAT, with a performance gain over Single-SIC of 3.8 bps/Hz at $P_J = 0.1W$ and that decreases with P_J. It should be noted that, even though we presented results with P_J reaching a maximum value of 10W, the majority of commercial jammers are low-power jammers that usually operate in the range of a few watts, and seldom exceed 5W.

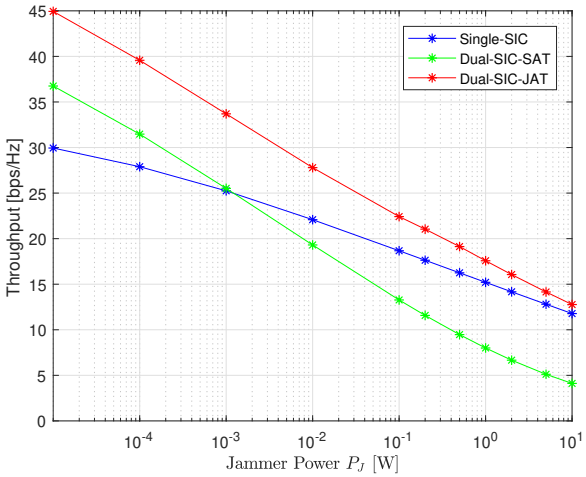

Fig. 5: Sum-throughput versus P_J for $P_L = 1$W

In Fig. 6, we represent the average sum-throughput obtained by varying the total system transmit power, for $P_J = 0.1$ and 1W. One can observe how the performance gain of Dual-SIC-JAT over Single-SIC increases with P_L, for example from 1.9 bps/Hz at $P_L = 0.5W$ to 3.7 bps/Hz at $P_L = 10W$, for $P_J = 1W$. When $P_J = 0.1W$, the performance loss of Dual-SIC-SAT vs. Single-SIC decreases from 6 bps/Hz at $P_L = 0.5W$ to 2.8 bps/Hz at $P_L = 10W$.

Table I shows examples of the obtained optimum sum-throughput for two different configurations of users and jam-

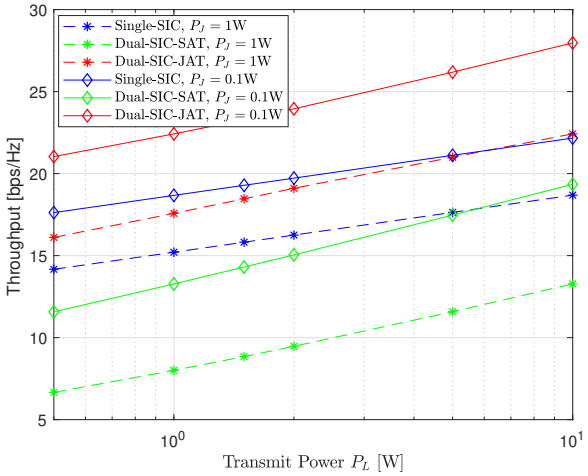

Fig. 6: Sum-throughput versus P_L for $P_J = 0.1$ and 1W

mer positions, as well as the selected RRHs and subbands. The first example considers users U12 and U41, one in a room and the other nearby in the corridor (Cf. Fig. 3), in the presence of the Jammer J4, which is relatively close to both users, with $P_J = 0.2$W and $P_L = 1$W. The Single-SIC technique selects the best RRH41, which is in the same room as U41 and also close to U12. Dual-SIC-SAT selects RRH41 and RRH102, and Dual-SIC-JAT selects RRH12 and RRH41, i.e., one of the serving RRHs is the same as in Single-SIC, while the second one is relatively close to both users. The gain of Dual-SIC-JAT over Single-SIC is 4.9bps/Hz, while Single-SIC outperforms Dual-SIC-SAT by 2.4bps/Hz. In the second example, we consider two users U51 and U101 from two different rooms on the two sides of the corridor, in the presence of J3 from room #8, i.e. more distanced from the users than in the first example. Now $P_J = 1W$. Again, the Single-SIC method selects an RRH in the same room as one of the users. This time, Dual-SIC-SAT, which selects one RRH (RRH91) in a different but close room and the other one in the same room (RRH102) as one user, outperforms Single-SIC by 2.7 bps/Hz. Dual-SIC-JAT, which selects the RRHs in the two rooms where the users are located, outperforms Dual-SIC-SAT and Single-SIC by 6.1 and 8.8 bps/Hz respectively. These examples clearly show that Dual-SIC-SAT can sometimes outperform Single-SIC. Therefore, the choice between the three methods should be done adaptively, depending on the users positions and jamming conditions, as well as the affordable resource allocation complexity.

k_1, k_2, J	SIC	Rate	RRHs	Subband
U12, U41, J4	Single	11.2	RRH41	12
	Dual-SAT	8.8	RRH41, RRH102	12
	Dual-JAT	16.1	RRH12, RRH41	7
U51, U101, J3	Single	14.8	RRH51	8
	dual SAT	17.5	RRH102, RRH91	5
	dual JAT	23.6	RRH102, RRH51	5

TABLE I: Examples of the obtained optimum rates [bps/Hz], RRHs and subbands, for $P_J = 0.2W$ (first example) and 1W (second example) and $P_L = 1W$

In Table II, the influence of the jammer deployment on a fixed user set (U51, U101) is shown, for the Dual-SIC-JAT method, with $P_J = 1$W and $P_L = 1$W. Among the 5 jammer positions, the J4 position turns out to be the most dramatic one for this user couple. Indeed, J4 is relatively close to both users and the worst throughput is achieved, while the best RRHs selected to counteract its effect are RRH51 and RRH121, one in the same room as U51 and the other rather away from both users. A close maximum throughput is achieved when J2 is deployed, which is very close to U51. In this case, the two selected RRHs are in the same room as the other user. The jammer that has the least incidence on throughput is J3, since it is relatively far from both users. In this case, each of the selected RRHs is in the same room as one of the users. The same couple of RRHs is selected when jammer J1 is deployed, which is also relatively far from the users. This analysis shows the importance of taking into account the jammer position in the RRH and subband selection procedure, since particular RRH patterns appear depending on the jammer-users configuration.

k_1, k_2	J	Rate	RRHs	Subband
U51, U101	J1	13.5	RRH51, RRH102	12
	J2	6.8	RRH101, RRH102	1
	J3	25.6	RRH51, RRH102	5
	J4	5.3	RRH51, RRH121	12
	J5	15.4	RRH13, RRH51	12

TABLE II: Optimum rates [bps/Hz], RRHs and subbands, obtained by Dual-SIC-JAT, for a particular user couple, with the different Jammer positions, for $P_J = 1W$ and $P_L = 1W$.

VII. Conclusion

In this paper, three user-pairing strategies were proposed in the NOMA-DAS setting, in the aim of alleviating the influence of a jammer on downlink transmissions. Practical channel measurements were taken in an indoor environment, with a large number of users, antennas, and jammer positions. The theoretical foundations were developed for the three pairing strategies and incorporated in a subband and RRH selection technique. The results of this study show that, in contrast with those of previous works performed in a jamming-free NOMA-DAS context, the best pairing strategy greatly depends on the users positions and jamming conditions (jammer position and power). An adaptive choice between the three strategies should therefore be conducted so as to optimize the system performance. This study, performed in the DAS context, can also be directly applied to CoMP transmissions in multi-cell systems using joint transmission (JT) or dynamic point selection (DPS) [28].

References

[1] Z. Zhu, S. Huang, Z. Chu, F. Zhou, D. Zhang, and I. Lee, "Robust Designs of Beamforming and Power Splitting for Distributed Antenna Systems With Wireless Energy Harvesting," *IEEE Systems Journal*, vol. 13, no. 1, pp. 30–41, March 2019.

[2] C. He, Y. Zhou, G. Qian, X. Li, and D. Feng, "Energy efficient power allocation based on machine learning generated clusters for distributed antenna systems," *IEEE Access*, vol. 7, pp. 59 575–59 584, 2019.

[3] X. Yu, W. Xu, S.-H. Leung, Q. Shi, and J. Chu, "Power Allocation for Energy Efficient Optimization of Distributed MIMO System With Beamforming," *IEEE Trans. on Veh. Tech.*, vol. 68, no. 9, pp. 8966–8981, 2019.

[4] H. Ren, N. Liu, C. Pan, and C. He, "Energy Efficiency Optimization for MIMO Distributed Antenna Systems," *IEEE Trans. on Veh. Tech.*, vol. 66, no. 3, pp. 2276–2288, March 2017.

[5] C. Pan, H. Zhu, N. J. Gomes, and J. Wang, "Joint Precoding and RRH Selection for User-Centric Green MIMO C-RAN," *IEEE Trans. on Wir. Comm.*, vol. 16, no. 5, pp. 2891–2906, 2017.

[6] Z. Zhu, K.-J. Lee, Z. Wang, and I. Lee, "Robust Beamforming and Power Splitting Design in Distributed Antenna System with SWIPT under Bounded Channel Uncertainty," in *2015 IEEE 81st Veh. Tech. Conf. (VTC Spring)*, 2015, pp. 1–5.

[7] A. Benjebbour, A. Li, Y. Saito, Y. Kishiyama, A. Harada, and T. Nakamura, "System-level Performance of Downlink NOMA for Future LTE Enhancements," in *Globecom Workshops*. IEEE, 2013, pp. 66–70.

[8] Z. Ding, Z. Yang, P. Fan, and H. V. Poor, "On the Performance of Non-Orthogonal Multiple Access in 5G Systems with Randomly Deployed Users," *IEEE Signal Process. Lett.*, vol. 21, no. 12, pp. 1501–1505, Dec. 2014.

[9] M.-R. Hojeij, J. Farah, C. A. Nour, and C. Douillard, "Resource Allocation in Downlink Non-Orthogonal Multiple access (NOMA) for Future Radio Access," in *IEEE 81st Veh. Tech. Conf. (VTC Spring)*, 2015, pp. 1–6.

[10] J. Farah, E. Sfeir, C. Abdel Nour, and C. Douillard, "New Resource Allocation Techniques for Base Station Power Reduction in Orthogonal and Non-Orthogonal Multiplexing Systems," in *2017 IEEE Int. Conf. on Commun. Workshops (ICC Workshops)*, May 2017, pp. 618–624.

[11] S. Han, X. Xu, X. Tao, and P. Zhang, "Joint Power and Sub-Channel Allocation for Secure Transmission in NOMA-Based mMTC Networks," *IEEE Systems Journal*, vol. 13, no. 3, pp. 2476–2487, Sep. 2019.

[12] J. Lu, Y. Wang, T. Liu, Z. Zhuang, X. Zhou, F. Shu, and Z. Han, "UAV-Enabled Uplink Non-Orthogonal Multiple Access System: Joint Deployment and Power Control," *arXiv preprint arXiv:1908.09289*, 2019.

[13] A. Kilzi, J. Farah, C. Abdel Nour, and C. Douillard, "Mutual Successive Interference Cancellation Strategies in NOMA for Enhancing the Spectral Efficiency of CoMP Systems," *IEEE Trans. on Commun.*, vol. 68, no. 2, pp. 1213–1226, Feb 2020.

[14] J. Farah, A. Kilzi, C. Abdel Nour, and C. Douillard, "Power Minimization in Distributed Antenna Systems Using Non-Orthogonal Multiple Access and Mutual Successive Interference Cancellation," *IEEE Trans. on Veh. Technol.*, vol. 67, no. 12, pp. 11 873–11 885, Dec. 2018.

[15] J. Zhu, J. Wang, Y. Huang, S. He, X. You, and L. Yang, "On Optimal Power Allocation for Downlink Non-Orthogonal Multiple Access Systems," *IEEE J. Sel. Areas Commun.*, vol. 35, no. 12, pp. 2744–2757, Dec 2017.

[16] X. Gu, X. Ji, Z. Ding, W. Wu, and M. Peng, "Outage Probability Analysis of Non-Orthogonal Multiple Access in Cloud Radio Access Networks," *IEEE Commun. Lett.*, vol. 22, no. 1, pp. 149–152, Jan 2018.

[17] K. N. Pappi, P. D. Diamantoulakis, and G. K. Karagiannidis, "Distributed Uplink-NOMA for Cloud Radio Access Networks," *IEEE Commun. Lett.*, vol. 21, no. 10, pp. 2274–2277, Oct 2017.

[18] M. J. Youssef, J. Farah, C. Abdel Nour, and C. Douillard, "Resource Allocation for Mixed Traffic Types in Distributed Antenna Systems Using NOMA," in *2018 IEEE 77th Veh. Technol. Conf. (VTC fall)*, Aug. 2018, pp. 1–5.

[19] M. Youssef, J. Farah, C. A. Nour, and C. Douillard, "Resource Allocation in NOMA Systems for Centralized and Distributed Antennas With Mixed Traffic Using Matching Theory," *IEEE Trans. on Commun.*, vol. 68, no. 1, pp. 414–428, Jan 2020.

[20] A. Kilzi, J. Farah, C. A. Nour, and C. Douillard, "New Power Minimization Techniques in Hybrid Distributed Antenna Systems With Orthogonal and Non-Orthogonal Multiple Access," *IEEE Trans. Green Commun. Netw.*, vol. 3, no. 3, pp. 679–690, Sep. 2019.

[21] V. Deniau, C. Gransart, G. L. Romero, E. P. Simon, and J. Farah, "IEEE 802.11n Communications in the Presence of Frequency-Sweeping Interference Signals," *IEEE Trans. on Electromagnetic Compatibility*, vol. 59, no. 5, pp. 1625–1633, Oct 2017.

[22] K. Grover, A. Lim, and Q. Yang, "Jamming and Anti-Jamming Techniques in Wireless Networks: a Survey," *Int. Journal of Ad Hoc and Ubiquitous Computing*, vol. 17, no. 4, pp. 197–215, 2014.

[23] J. Farah, J. Akiki, and E. P. Simon, "Energy-Efficient Techniques for Combating the Influence of Reactive Jamming Using Non-Orthogonal Multiple Access and Distributed Antenna Systems," in *2019 Wireless Telecom. Symposium (WTS)*, April 2019, pp. 1–7.

[24] E. P. Simon, J. Farah, and P. Laly, "Performance Evaluation of Massive MIMO With Beamforming and Nonorthogonal Multiple Access Based on Practical Channel Measurements," *IEEE Antennas and Wireless Propagation Letters*, vol. 18, no. 6, pp. 1263–1267, June 2019.

[25] R. Heath, S. Peters, Y. Wang, and J. Zhang, "A Current Perspective on Distributed Antenna Systems for the Downlink of Cellular Systems," *IEEE Commun. Mag.*, vol. 51, no. 4, pp. 161–167, April 2013.

[26] W. Choi and J. G. Andrews, "Downlink Performance and Capacity of Distributed Antenna Systems in a Multicell Environment," *IEEE Trans. on Wir. Commun.*, vol. 6, no. 1, pp. 69–73, Jan 2007.

[27] "Physical Layer Aspects for Evolved UTRA, TR25-814 (V7.1.0)," 3GPP, Tech. Rep., 2006.

[28] E. Pateromichelakis, M. Shariat, A. u. Quddus, and R. Tafazolli, "On the Evolution of Multi-Cell Scheduling in 3GPP LTE / LTE-A," *IEEE Commun. Surveys Tutorials*, vol. 15, no. 2, pp. 701–717, Second 2013.

Joumana Farah received the B.E. degree in Electrical Engineering from the Lebanese University, in 1998, the M.E. degree in Signal, Image, and Speech processing, in 1999, and the Ph.D. degree in mobile communication systems, in 2002, from the University of Grenoble, France. In 2010, she received the Habilitation to Direct Research (HDR) from University Pierre and Marie Curie (Paris VI), France. She is currently a full-time professor at the Faculty of Engineering, Lebanese University, Lebanon. She has supervised a large number of Master, PhD theses and post-docs. She has received several research grants from the Lebanese National Council for Scientific Research, the Franco-Lebanese CEDRE program, and the Lebanese University. She has nine registered patents and a software and has coauthored a research book and more than a hundred of papers in international journals and conferences. Her current research interests include resource allocation techniques, channel coding, channel estimation, and interference management techniques. She was the General Chair of the 19th International Conference on Telecommunications (ICT 2012), and serves as a TPC member and a reviewer for several journals and conferences.

Eric P. Simon received the Master's degree in electronics engineering from the Superior School of Electronics (ESCPE), Lyon, France, in 1999, and the Ph.D. degree in signal processing and communications from the National Polytechnic Institute of Grenoble (INPG), France, in 2004. During 2005, he was a Teaching Assistant at the INPG and the following year he joined one of France Telecom R&D Laboratories as a Postdoctoral Fellow. He is currently an Associate Professor at the Institute of Electronics, Microelectronics and Nanotechnology (IEMN), TELICE (Telecommunications, Interference and Electromagnetic Compatibility) group, University of Lille, France. In 2015, he received the Accreditation for Research Supervision (HDR) from University of Lille. His main research interests are in signal detection and estimation, multicarrier, and multiple-access communication systems.

Pierre Laly is a study engineer at the University of Lille, France. His main current research areas are the study, design and realization of electronic cards to build prototypes dedicated to digital and/or analog telecommunication systems. He works on the implementation and programming of microcontrollers, DSP, CPLD, FPGA components, and on the implementation of sub-systems for the recovery and the statistical treatment of the various prototypes information. He also handles the maintenance and installation of computer equipment of TELICE (Telecommunications, Interference and Electromagnetic Compatibility) Group, at the University of Lille.

Gauthier Delbarre is an assistant engineer at the University of Lille, France. He takes part in the field measurement campaigns of propagation channels conducted with the TELICE (Telecommunications, Interference and Electromagnetic Compatibility) group as technical support for researchers. His current projects are the realization and automation of electromagnetic compatibility (EMC) measurements, as well as fault detection in wired networks. He also produces prototypes of electronic cards for TELICE, the University of Lille, and various start-ups.